

# Structure and Conducting Properties of $\text{La}_{1-x}\text{Sr}_x\text{CoO}_{3-\delta}$ Films

X. Chen,\* N. J. Wu and A. Ignatiev

Space Vacuum Epitaxy Center and Texas Center for Superconductivity, University of Houston, Houston, TX 77024-5507, USA

## Abstract

$\text{La}_{1-x}\text{Sr}_x\text{CoO}_{3-\delta}$  (LSCO) films have been deposited on  $\text{LaAlO}_3$  (LAO),  $\text{La}_{1-x}\text{Sr}_x\text{Ga}_{1-y}\text{Mg}_y\text{O}_{3-\delta}/\text{LaAlO}_3$  (LSGM/LAO) and yttria-stabilized zirconia (YSZ) substrates by pulsed laser deposition (PLD) for application to thin film solid oxide fuel cell cathodes. The optimum conditions for deposition were determined for the different substrates in an ambient of 80–310 mTorr oxygen pressure and at a substrate temperature range of 450 to 750°C. The films structures were analyzed by XRD, RBS and SEM. Epitaxial LSCO films were grown with (110) preferred orientation on YSZ, and with (100) orientation on LAO and LSGM/LAO. The electrical resistivity of the epitaxial LSCO films ranged from  $10^{-2}$  to  $10^{-4}$   $\Omega$  cm, depending on the deposition temperature and substrate. The ionic conducting behavior of the LSCO film on YSZ was investigated by impedance measurement. © 1999 Elsevier Science Limited. All rights reserved

**Keywords:** films, surfaces, impedance, fuel cells.

## 1 Introduction

The electronic and ionic conductor  $\text{La}_{0.5}\text{Sr}_{0.5}\text{CoO}_{3-\delta}$  (LSCO) is an important cathode material for solid oxide fuel cells (SOFC).<sup>1–5</sup> Recently, PLD<sup>6</sup> has been used to fabricate LSCO thin films for application to SOFC,<sup>7</sup> however much work is still required for realizing integrated thin film SOFC. Using integrated oxide thin films for fuel cell design can reduce the size and cost of cells. Particularly, a simple planar thin film structure for the fuel cells is expected to work at a lower operating temperature than bulk cells due to a higher projected efficiency of ion transport.

LSCO is a perovskite-type oxide<sup>8</sup> with a low electrical resistivity. It is also an oxygen ion conductor, and as a result, is used as a fuel cell cathode material. An oxygen ion conductor that is an electronic insulator is used in bulk form as a fuel cell electrolyte material. A solid oxide fuel cell, therefore, typically consists of an LSCO cathode, an electrolyte, such as yttria-stabilized zirconia (YSZ) or  $\text{La}_{1-x}\text{Sr}_x\text{Ga}_{1-y}\text{Mg}_y\text{O}_{3-\delta}$  (LSGM), and a metallic anode (usually nickel). Such a fuel cell typically works at high temperature ( $\geq 800^\circ\text{C}$ ), and hence has degradation due to interface reactions and thermal expansion coefficient differences between LSCO and the electrolyte. It is expected that by using a thin film planar cell structure, the working temperature of the cell can be significantly reduced due to higher ionic transport, and hence the stability and performance of the cell can be improved.

In this paper, we have studied the structure and conducting properties of the LSCO thin films deposited by PLD.

## 2 Experimental

LSCO films have been deposited on  $\text{LaAlO}_3$  (LAO),  $\text{La}_{1-x}\text{Sr}_x\text{Ga}_{1-y}\text{Mg}_y\text{O}_{3-\delta}/\text{LaAlO}_3$  (LSGM/LAO) and YSZ substrates by PLD. A KrF excimer laser was used at an energy of 0.190 J/pulse (fluence =  $1.25\text{ Jcm}^{-2}$ ), and a frequency of 7 Hz. The target was a commercially obtained, sintered LSCO pellet mounted on a rotating holder in a vacuum chamber with base pressure of  $2 \times 10^{-5}$  torr. The substrate was a (100) YSZ single crystal wafer mounted on a halogen lamp heated holder allowing for growth temperatures ranging from room temperature to 1000°C. The LSCO films were deposited in an oxygen ambient at pressures from 80 to 310 mTorr. The substrate temperature was varied from 450 to 750°C for the growths. Film crystal structure was analyzed by X-ray diffraction (XRD). XRD 2 $\theta$  scans were collected with a Siemens D-5000 system. Additional XRD analysis

\*To whom correspondence should be addressed. Fax: +1-713-747-7724; e-mail: xinchen73@hotmail.com

was performed with a Siemens General Area Detector Diffraction System (GADDS). SEM and EDS were also used for determination of both morphology and general composition of the samples. LSCO film resistivity was measured by the traditional four-probe method using sputter-deposited silver contacts.

A LSCO/YSZ/LSCO testing cell was made by depositing LSCO films on two sides of a YSZ wafer. The AC impedance of the cell at high temperature was measured with an Impedance/Gain Phase Analyzer.

### 3 Results

#### 3.1 LSCO on LAO

LAO is a perovskite-type oxide, with a lattice parameter similar to LSCO. Deposition of LSCO on LAO substrates at high temperatures ( $\geq 550^\circ\text{C}$ ) yields epitaxial films. Figure 1(1) is the XRD  $2\theta$  analysis of a LSCO film deposited at  $650^\circ\text{C}$  on a LAO (100) substrate. We can see a strong LSCO (200) peak only, indicating a good (100) oriented film. SEM analysis on the film shows a generally smooth surface. XRD pole figure analysis shows a  $\Delta\phi$  of  $\sim 1^\circ$  on the film, RBS analysis shows a  $\chi_{\min}$  of 6%, indicating a good epitaxial film. LSCO has also been deposited on LSGM/LAO substrates. A good epitaxial film is also grown [Fig. 1(2)].

#### 3.2 LSCO on YSZ

LSCO films were also deposited on YSZ (100) substrates at 450 to  $750^\circ\text{C}$ . YSZ has a crystal structure different from that of LSCO. When deposited at  $750^\circ\text{C}$  in a 150 mTorr oxygen ambient, a smooth (110) oriented LSCO film is developed on the YSZ (100) substrate, which is shown by SEM and XRD measurements [Fig. 1(3)]. XRD pole figure analysis shows a  $\Delta\phi$  of  $\sim 10^\circ$ , and RBS

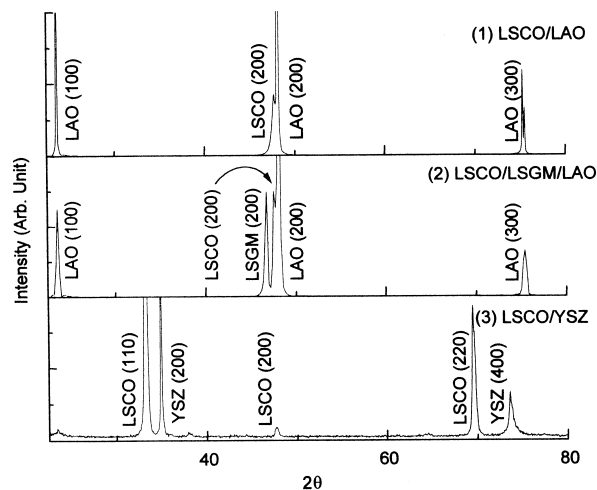


Fig. 1. XRD  $2\theta$  analysis of LSCO thin films deposited by PLD.

analysis shows a  $\chi_{\min}$  of 30%, indicating the film is highly oriented poly-crystal.

When deposited at  $650^\circ\text{C}$ , the (110) diffraction is weakened, and a strong LSCO (100) diffraction peak appears, indicating a mainly (100) oriented film. Upon further decreasing the deposition temperature to  $550^\circ\text{C}$ , the film again becomes (110) oriented. Detailed XRD analysis by GADDS measurement shows that in difference to the  $750^\circ\text{C}$  deposited highly oriented film, the  $550^\circ\text{C}$  deposited film shows many different crystal orientation directions. The fraction of (110) oriented crystallites in the  $550^\circ\text{C}$  deposited film is larger than the other crystal orientations, so that a (110) diffraction peak appears in the XRD  $2\theta$  scan. The LSCO diffraction peaks from the  $450^\circ\text{C}$  deposited film are very weak, indicating an amorphous film.

Figure 2(a) is an illustration of the LSCO lattice structure.<sup>7</sup> Site A is occupied by La or Sr atoms and site B is occupied by Co atoms. The large circles represent the oxygen atoms. The atom arrangements for the LSCO(110) and (100) planes are also shown in Fig. 2(a). Figure 2(b) is a lattice model of the YSZ unit cell. Zr or Y atoms are located at the corners and the face centers of the unit cell, with a cubic structure of eight oxygen atoms inside the cell. Previous work has shown that the exposed surfaces of oxides are usually oxygen terminated.<sup>9,10</sup> If the YSZ surface is fully covered

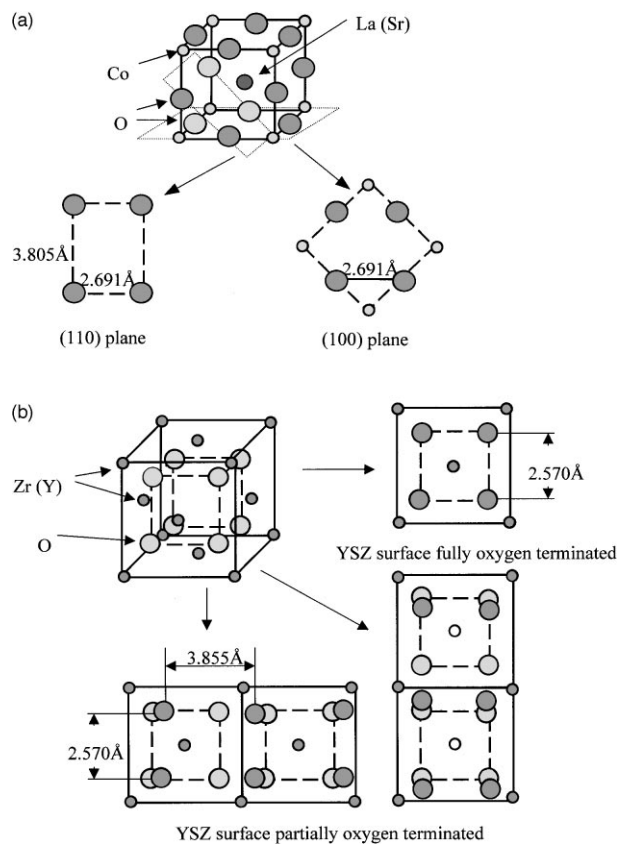


Fig. 2. A schematic model for the lattice match and film growth of LSCO on YSZ: (a) an illustration of LSCO lattice structure; (b) atomic model of the LSCO/YSZ surface.

with oxygen, the surface oxygen atom arrangement is similar to that of the LSCO (100) plane indicated in Fig. 2(a), and (100) oriented LSCO growth is expected. If the YSZ surface does not have full oxygen coverage, then with the presence of surface oxygen vacancies a surface oxygen arrangement similar to that in the LSCO (110) plane could be realized, resulting in (110) oriented growth for LSCO.

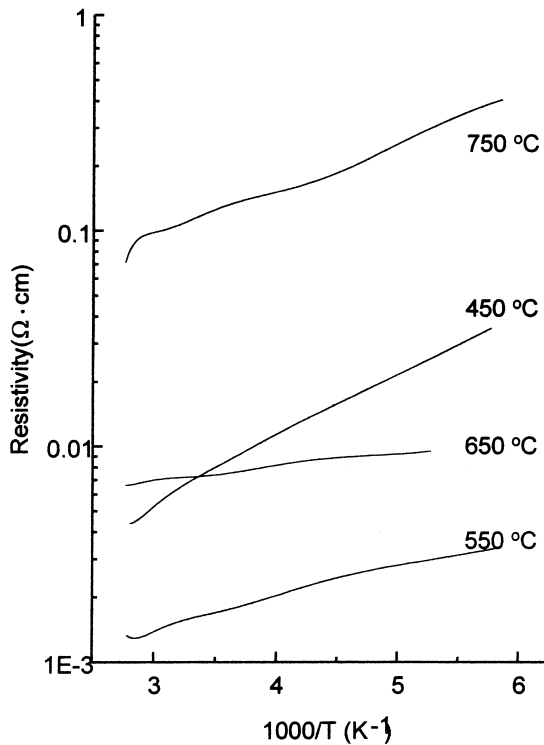


Fig. 3. Resistivity of LSCO/YSZ films with different deposition temperatures.

This surface oxygen model can explain the observed LSCO thin film growth on YSZ substrate. At 650°C and under 150 m torr oxygen pressure, the YSZ surface is mostly covered with oxygen atoms. The YSZ surface oxygen atom arrangement matches that of the LSCO (100) plane, and (100) oriented LSCO films are grown.

When the substrate temperature is increased, the YSZ surface has oxygen vacancies, and a (110) oriented LSCO film is likely to develop on the YSZ surface. When the deposition temperature is decreased to 550°C, LSCO crystals with various directions can grow on the surface. Consider the boundary between the film and the substrate. For a (110) oriented LSCO grain on the YSZ substrate, the crystal mismatch at one side is very small, only 1.3%, while mismatch at the other side is 4.7%. For an (100) oriented grain, the mismatch with the substrate is larger, 4.7% for both sides. When crystals with different orientations grow together and compete with each other, a (110) oriented grain is therefore expected to be more stable with respect to lattice mismatch, and therefore more likely to grow larger than (100) grain. As a result, a poly-crystalline but mostly (110) oriented film will be formed. When the deposition temperature is further decreased to 450°C, the film is not crystalline.

Changing the ambient oxygen pressure for the film deposition should similarly affect the surface oxygen concentration, and hence the structure of the film. This is supported by XRD analysis of the films deposited at 650°C in oxygen ambient from 80 to 310 m Torr, showing (100) film growth at higher oxygen pressures.

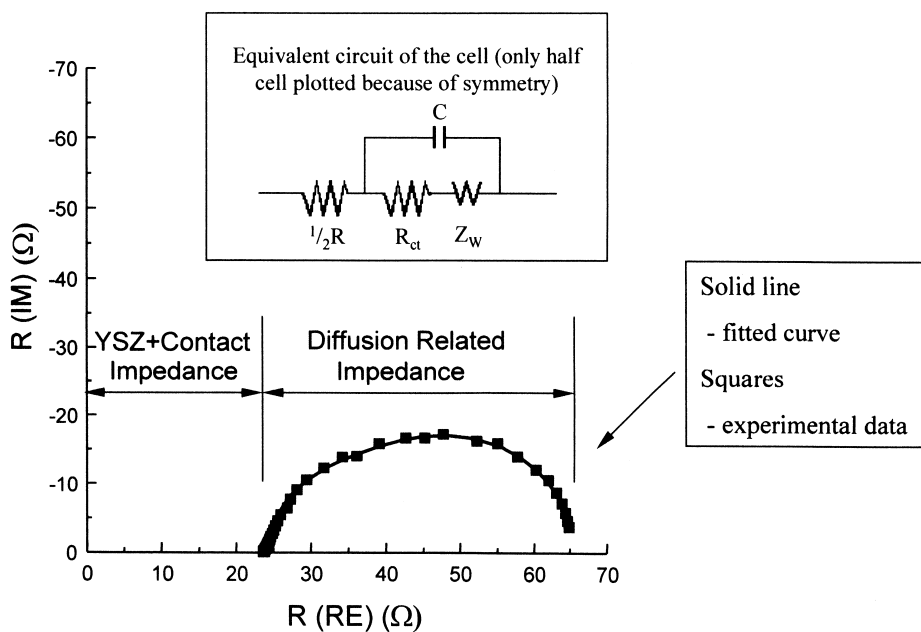


Fig. 4. Impedance of a LSCO/YSZ/LSCO test cell measured at 673°C; and an equivalent circuit used to analyze the impedance of the test cell.

The measured resistivity of the LSCO films is shown in Fig. 3. The lowest resistivity from the LSCO film deposited on YSZ is  $1 \times 10^{-3} \Omega \text{ cm}$  at 300 K for the  $550^\circ\text{C}$  deposited film.

### 3.3 LSCO/YSZ/LSCO

A LSCO/YSM/LSCO test cell was made by deposition of LSCO on the two sides of a YSZ wafer. Its AC impedance was measured and the impedance spectrum is shown in Fig. 4. The semicircle is an impedance which is related to oxygen diffusion at the sample surface. The lower intercept of the semicircle is the sum of YSZ and sample contact impedance. The equivalent circuit model<sup>11</sup> for the test cell is inserted in Fig. 4. For the circuit,  $R_{ct}$  is the charge transfer resistance,  $C$  is the air/sample interface capacitance, and  $Z_w$  is the Warburg impedance which is given by:<sup>12</sup>

$$Z_w = R_{mt} \frac{\tanh \sqrt{j\omega t_w}}{\sqrt{j\omega t_w}} \quad (1)$$

where  $R_{mt}$  is mass transfer resistance and  $t_w$  is a time constant defined by:

$$t_w = l_c^2/D \quad (2)$$

where  $l_c$  is the thickness of the diffusion layer which might be the thickness of the LSCO layer and  $D$  is the diffusion coefficient.

The impedance spectrum has been fitted by the equivalent circuit model, yielding a  $t_w$  value of 0.84 s. With an LSCO film thickness of  $0.31 \mu\text{m}$ , the diffusion coefficient of the film is estimated to be  $1.1 \times 10^{-9} \text{ cm}^2 \text{ s}^{-1}$  which is somewhat lower than values given in the literature.<sup>13</sup> DC polarization analysis of the cell is underway.

## 4 Conclusion

Epitaxial LSCO films have been deposited on LAO and LSGM/LAO substrates. The crystal orientations of LSCO films deposited on YSZ are different when deposited at different temperatures and under different oxygen ambient pressures. The lowest resistivity of  $1 \times 10^{-3} \Omega \text{ cm}$  for LSCO film on YSZ is obtained when deposited at  $550^\circ\text{C}$  under 150 mTorr oxygen pressure. The main part of the

impedance of a LSCO/YSZ/LSCO testing cell is contributed by diffusion impedance.

## Acknowledgements

The assistance of A. Jacobson, Y. L. Yang, S. Wang and Z. H. Zhang is greatly acknowledged. This work was partially supported by the MRSEC Program of the National Science Foundation under award number DMR-9632667, NASA; the Texas Advanced Technology Program under grant number 003652-059; and the R. A. Welch Foundation.

## References

1. Minh, N. Q., Ceramic fuel cells. *J. Am. Ceram. Soc.*, 1993, **76**(3), 563–588.
2. Itoh, N., Kato, T., Uchida, K. and Haraya, K. Preparation of pore-free disk of  $\text{La}_{1-x}\text{Sr}_x\text{CoO}_3$  mixed conductor and its oxygen permeability. *J. Membrane Sci.* 1994, **92**, 239–246.
3. Petrov, A. N., Kononchuk, O. F., Andreev, A. V., Cherepanov, V. A. and Kofstad, P. Crystal structure, electrical and magnetic properties of  $\text{La}_{1-x}\text{Sr}_x\text{CoO}_{3-y}$ . *Solid State Ionics* 1995, **80**, 189–199.
4. Mizusaki, J., Tabuchi, J., Matsuura, T., Yamauchi, S. and Fueki, K. Electrical conductivity and seebeck coefficient of nonstoichiometric  $\text{La}_{1-x}\text{Sr}_x\text{CoO}_{3-\delta}$ . *J. Electrochem. Soc.* 1989, **136**(7), 2082–2088.
5. Kawada, T. and Yokokawa, H. Materials and characterization of solid oxide fuel cell. *Key Engineering Mater.*, 1997, **125–126**, 187–248.
6. Smith, D. L. *Thin-Film Deposition: Principles and Practice*, McGraw-Hill, New York, 1995, 394–400.
7. Coccia, L. G., Tyrrell, G. C., Kilner, J. A., Waller, D., Chater, R. J., and Boyd, I. W., Pulsed laser deposition of novel materials for thin film solid oxide fuel cell applications:  $\text{Ce}_{0.9}\text{Gd}_{0.1}\text{O}_{1.95}$ ,  $\text{La}_{0.7}\text{Sr}_{0.3}\text{CoO}_y$  and  $\text{La}_{0.7}\text{Sr}_{0.3}\text{Co}_{0.2}\text{Fe}_{0.8}\text{O}_y$ . *Appl. Surf. Sci.* 1996, **96–98**, 795–801.
8. Ohbayashi, H., Kudo, T. and Gejo, T. Crystallographic, electric and thermochemical properties of the perovskite-type  $\text{Ln}_{1-x}\text{Sr}_x\text{CoO}_3$  (Ln: Lanthanoid element). *Japanese J. of Appl. Phys.*, 1974, **13**, 1–7.
9. Taylor, T. N. and Ellis, W. P. Distorted surface oxygen structure on  $\text{UO}_2$  (100). *Surface Sci.* 1981, **107**, 249–262.
10. Ellis, W. P. and Taylor, T. N.  $\text{He}^+$  Ion-scattering spectroscopy studies of  $\text{UO}_2$  (*hkl*) Surfaces. *Surface Sci.* 1980, **91**, 409–422.
11. Liu, M., private communication.
12. Macdonald, J. R. *Impedance Spectroscopy: Emphasizing Solid Materials and Systems*, John Wiley & Sons, New York, 1987, 88.
13. Adler, S. B., Lane, J. A. and Steele, B. C. H. Electrode kinetics of porous mixed-conducting oxygen electrodes. *J. Electrochem. Soc.* 1996, **143**(11), 3554–3564.